Engineering-geology model of the seismically-induced Cerda landslide (Sicily, Italy)

F. Bozzano[1], E. Cardarelli[2], M. Cercato[2], L. Lenti[3], S. Martino[1], A. Paciello[4] and G. Scarascia Mugnozza[1]

[1] *Dip. Scienze della Terra - Università "La Sapienza", Roma and Centro di Ricerca sui Rischi Geologici, CERI, Valmontone, Italy*

[2] *Dip. Idraulica Trasporti e Strade, Università "La Sapienza", Roma, Italy*

[3] *Istituto Nazionale di Geofisica e Vulcanologia, Roma, Italy*

[4] *ENEA, Centro di Ricerca Casaccia, S.Maria di Galeria, Roma, Italy*

(Received: May 04, 2007; accepted: October 22, 2007)

ABSTRACT On September 6, 2002, a M_S=5.4 earthquake caused a large landslide close to the village of Cerda (Sicily, Italy) . The epicentre of the mainshock was located offshore, in the Tyrrhenian Sea, about 45 km NE of the city of Palermo and 50 km from the landslide site. The landslide involved an area of about 1.5 km^2 and caused significant damage to farmhouses, roads and aqueducts. The observed ground crack pattern pointed to a translational mechanism for the landslide, consistent with a sliding surface of up to 60 m b.g.l.. The sliding surface was recognised by two boreholes within the landslide mass, respectively at 10 and 30 m b.g.l.. The resulting stratigraphy showed a shallow 13-m-thick layer of weathered and remoulded clays and the landslide mass s.s., which involved softened scaly clays. The landslide mass was characterised by a large basal shear zone, composed by a 7-m-thick oxidised layer of scaly clays, including a 2-m-thick layer of completely remoulded and oxidised clays. Cross-hole seismic prospecting as well as seismometric measurements were carried out in order to better define the engineering-geology model and the elastic properties of the landslide mass. The S-wave profile inferred from cross-hole measurements showed a sharp velocity increase just below the sliding surface where high consistency and undisturbed scaly-clays were sampled. Amplification in the range 0.5-1 Hz comes from the ambient noise in a wide area within the landslide mass, corresponding to the upper portion of the slope; this effect could be related to the structural setting of the geological bedrock in the landslide area. On the other hand, amplification in the range 2.5-4.5 Hz can be referred to the local thickness of the landslide mass. The records of two weak motions confirm the evidence given by the ambient noise analysis.

1. Introduction

Defining the geological model of landslides is a problem frequently addressed using a multidisciplinary approach (Fookes *et al*., 2000; Havenith *et al*., 2002, 2003; Jongmans and Garambois, 2007). In order to define some geological constraints for the Cerda landslide, induced by the September 6, 2002 Palermo earthquake, geophysical investigations (seismic prospecting and seismometric measurements) together with geological surveys were carried out. Recently, integrated geophysical approaches, including both active and passive surface seismic

investigations as well as electromagnetic and electrical measurements, were proposed to analyse either the geometry or the dynamic properties of the landslide masses (Havenith *et al*., 2003; Meric *et al*., 2005). Some experiments on earthslides showed a consistent relation between the dynamic properties, the state of activity of landslides and the variation in S-wave velocity contrasts (Meric *et al*., 2007). In a recent review, Jongmans and Garambois (2007) discuss the importance of combining different geophysical methods and validating them using geotechnical information. This approach is aimed at defining a 3D engineering-geology model of the landslide, which is a fundamental tool for evaluating the associated risk for structures and infrastructures.

Seismic noise measurements, extensively applied to seismic zonation studies (Asten, 2004; Shapiro *et al*., 2005; Chavez-Garcia, 2007; Nunziata, 2007), once validated by different geological and geophysical investigations can be utilized to obtain a 3D engineering-geology model.

Seismic noise methodologies, however, have rarely been applied to landslide areas. The HVSRs from noise records were evaluated for the "Giarossa" large earthslide by Gallipoli *et al*. (2000) and combined with electrical tomographies; Meric *et al*. (2005) analyse the resonance effect of the "Séchilienne" rock-slide mass using noise records; Bordoni *et al*. (2006) report the findings of an experiment on the "Cavola" landslide to define the 3D wave propagation within the landslide mass. Meric *et al*. (2007) find a 1D resonance effect due to the "Super-Sauze" mudslide and to the "Saint-Guillaume" translational earthslide, using ellipticity and passive surface wave seismic investigastions. They also remark that: i) the observed resonance effects dramatically change in heterogeneous conditions within the landslide masses, especially where flow-like movements occur; ii) higher displacements along sliding surfaces generally correspond to higher seismic-wave velocity contrast and, consequently, to higher noise spectral amplitudes.

Effects of 2D resonance within landslide masses can be expected according to the critical shape ratio (Bard and Bouchon, 1985); some experiments show that 2D resonance effects in filled valleys can be obtained also from noise records (Steimen *et al*., 2003; Roten *et al.*, 2004). 2D and 3D site effects may also depend on high angle contacts in both symmetrical or asymmetrical basin-like systems (Mozco and Bard, 1993) as well as on fault zones (Rovelli *et al*., 2002). Some of these effects were observed from both noise and weak motion records (Martino *et al*., 2006).

Strong correlations between the occurrence of seismically-induced landslides and their epicentral distance as a function of both landslide type and earthquake magnitude are reported by several authors (Keefer, 1984; Rodriguez *et al*., 1999; Romeo, 2000).

2. The 2002 Cerda landslide reactivation

The September 6, 2002 earthquake (M_S=5.4) occurred in the Tyrrhenian Sea, about 45 km NE of Palermo, at a depth of about 10 km (Fig. 1). Although of moderate magnitude, the event locally produced strong effects in the city of Palermo, due to the high vulnerability of the buildings or unfavourable site conditions; 23 municipalities on the northern coast of Sicily and the nearby hinterland suffered slight damage (Azzaro *et al*., 2004).

The Cerda landslide is the main ground effect due to this earthquake; nevertheless, small falls were observed on the Island of Filicudi and some variations in discharge and temperature were

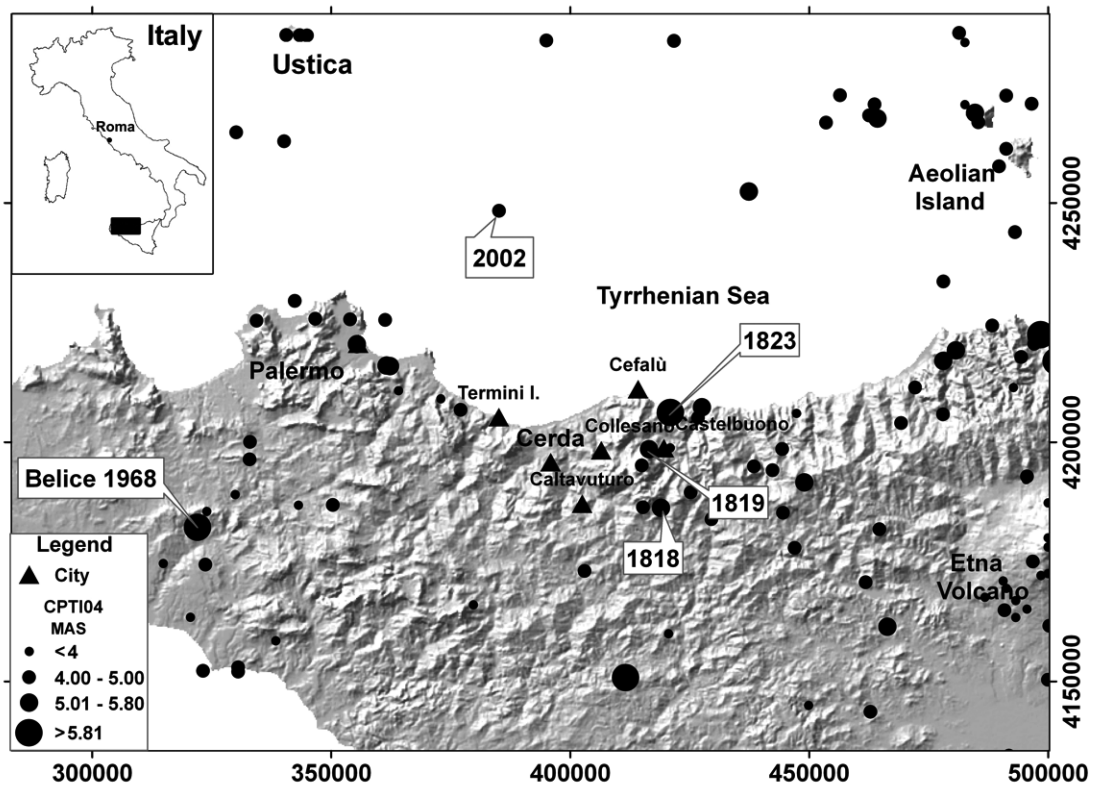

Fig. 1 - Historical seismicity in northern Sicily (by V. Verrubbi, ENEA Research Centre Casaccia, Roma, Italy); location of the Cerda village is also shown.

also recorded in the Termini Imerese springs as well as in the Alcamo thermal area (Azzaro *et al*., 2004).

The landslide involved an area of about 1.5 km^2 and was characterised by a main translational kinematism (Cruden and Varnes, 1996); it damaged many farmhouses, two aqueducts and some side roads. According to witnesses, the activation of the landslide took place about 30 minutes after the mainshock and, within a couple of hours, most of the cracks had significant horizontal and vertical offsets, that increased after the rainfall that occurred in the following 48 hours.

The induced ground crack pattern (Bonci *et al*., 2004), indicated a unitary movement and a low angle and "M shaped" main scarp (Fig. 2). Many longitudinal cracks were observed all over the middle slope portion of the landslide, as well as bulges and compressive cracks in the toe area (Fig. 3).

Mainly horizontal displacements were measured in the upper part of the slope up to 4-5 m, while mainly vertical displacements, up to 1 m, are measured at the bottom of the slope; a lot of minor ground cracks were rapidly deleted due to agricultural activities.

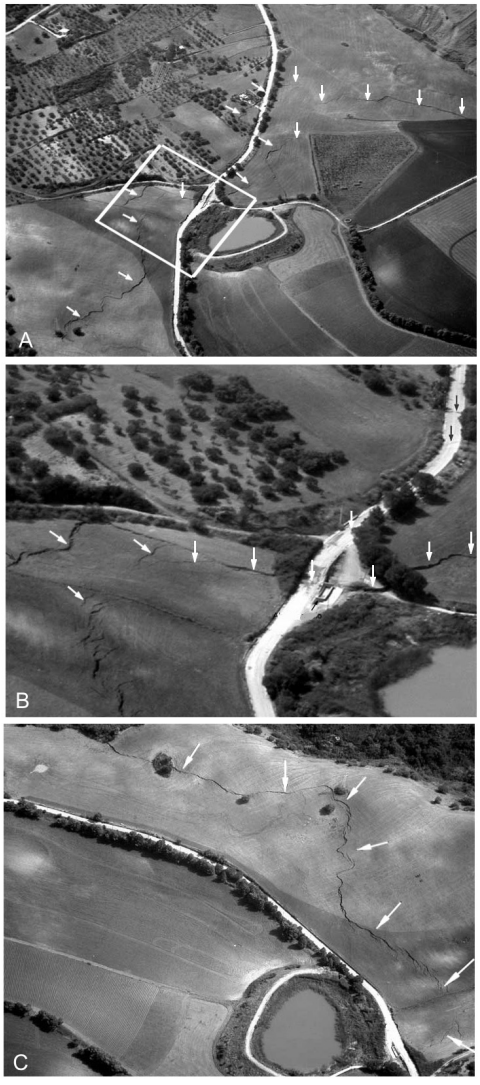

Fig. 2 - Aerial panoramic views of the Cerda landslide main scarp some days after the September 6, 2002 reactivation (by INGV): a) "M-shape" main scarp (the white square shows the area zoomed in Fig. 2b); b) secondary scarps and damage along a side road; c) detail of the main scarp (southeastern side).

3. Seismicity of the Cerda area

Macroseismic data available (CFTI3, 2000; DBMI04, 2004) for the village of Cerda and for some neighbouring towns (Fig. 1b), as well as local intensities estimated from CPTI04 (2004) and an attenuation relation for the Italian territory (Marcelli and Spadea, 1981) were taken into account in order to assess local seismicity at the site. Table 1 shows the intensities ≥ VI MCS felt or estimated in Cerda according to this analysis; when there are no observations in Cerda, felt data of nearby localities are reported.

The maximum intensity, historically observed at the site, is VII MCS, caused by the March 5, 1823 earthquake, which produced widespread damage all along the Tyrrhenian coast of Sicily. The 1823 macroseismic epicentre is placed on the coast; however recent data suggest (Gruppo di Lavoro, 2004) that the earthquake source could be located in a fault system E-W oriented, which extends west of the Aeolian arc as far as the Island of Ustica and which is also responsible for the September 6, 2002 event. Probably, most of the seismic events historically located along the coast had their actual epicentre in this offshore source.

There is no information about the effects in Cerda of the January 1693 eastern Sicily earthquakes (I=X-XI MCS), which "caused the largest seismic catastrophe in Sicilian history" (Azzaro *et al*., 2004). Intensity VII and V-VI MCS were respectively felt in Castelbuono and Cefalù, while variations in discharge or drainage of some springs are reported near Termini Imerese (CFTI3, 2000); according to these data and the estimated intensity in Table 1, the event should not have produced effects larger than VII MCS in Cerda. The earthquake source nearest to Cerda is the Madonie area, with epicentral distances of 20-30 km and M_{aw}= 5.3-5.4 (i.e. 1818 and 1819 events). Usually these earthquakes are felt in Termini Imerese, (with intensity ranging from IV to V MCS), but there are no observations in Cerda.

In summary, the site has no local seismicity; intensities not larger than VII MCS can be expected, mainly due to the Tyrrhenian offshore source.

Fig. 3 - Ground cracks within the landslide mass some days after the 6, September, 2002 reactivation (by the CERI team group): a, b) normal cracks in the active zone of the landslide; c) strike-slip crack in the neutral zone of the landslide; d) inverse crack in the passive zone of the landslide.

Table 1 - Earthquakes which produced felt ($\mathbf{I_{0ss}}$) or estimated ($\mathbf{I_S}$) macroseismic intensities ≥ VI in Cerda. Felt data in the area of neighbouring towns also reported.

year	month	day	epic.loc.	I_0 (MCS)	epic. dist. (km)	I_S (MCS)	I_{0SS} (MCS)
1693	1	11	East. Sicily	XI	137	VI-VI	VI Palermo, Castelbuono; V-VI Cefalù
1783	2	5	Calabria	XI	193	VI	
1818	9	8	Madonie	VII-VIII	25	VI	IV Termini Imerese
1819	2	24	Madonie	VII-VIII	21	VI	VII-VIII Collesano; VII Caltavuturo; VI Cefalù; V Termini Imerese
1823	3	5	North. Sicily	VIII-IX	27	VI-VII	VII Cerda
1908	12	28	Calabria	XI	164	VI	V Caltavuturo; IV Termini Imerese
1968	1	15	Belice	X	76	VI-VII	VI Cerda

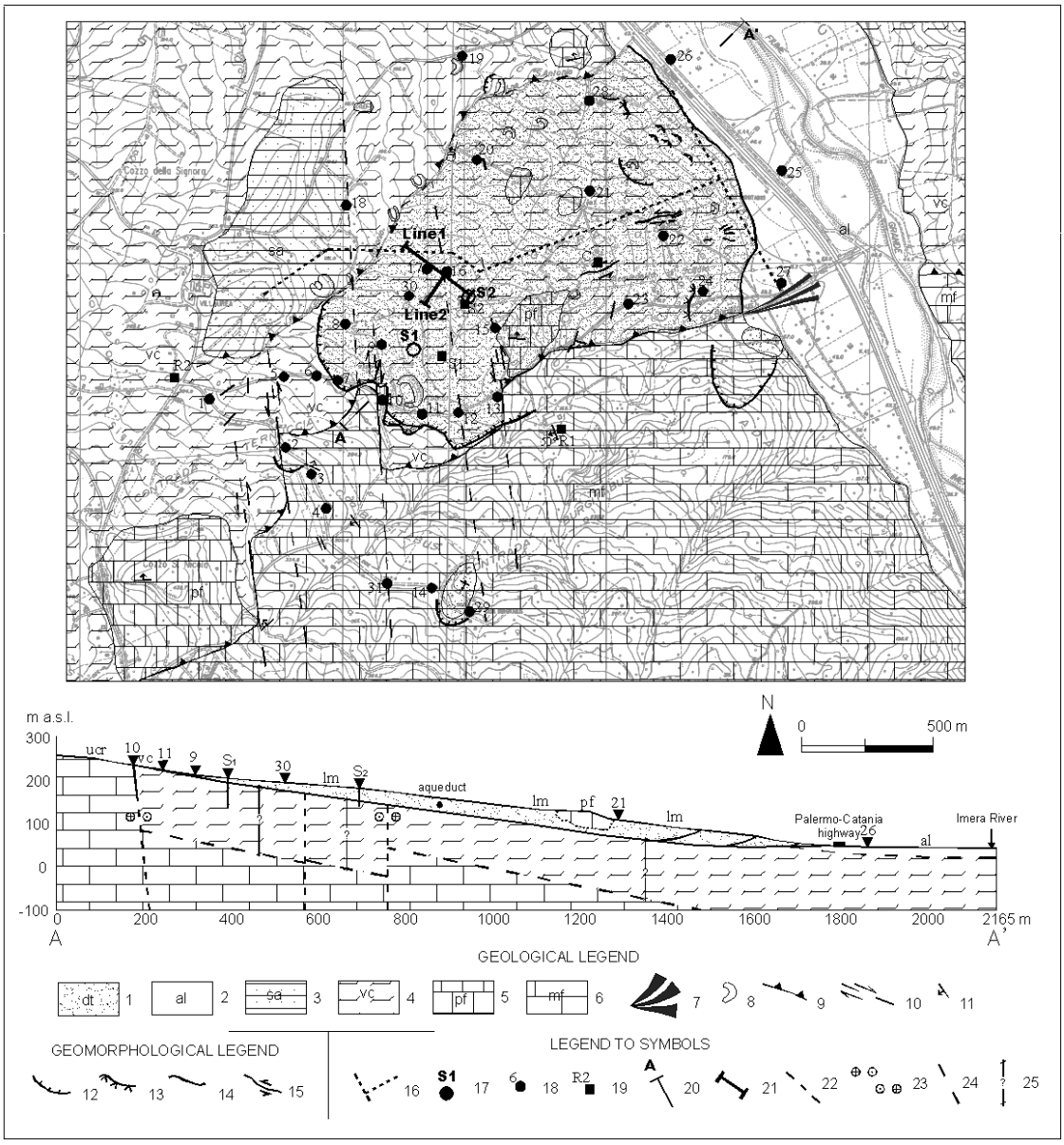

Fig. 4 - Geological map of the landslide area: 1) landslide mass; 2) alluvial deposits of the Imera River; 3) sandstones and sands of the Villaura Formation (Upper Miocene - Pliocene); 4) scaly clays of the Argille Varicolori Formation (Cretaceous – Eocene); 5) calcarenites of the Polizzi Formation (Eocene – Oligocene); 6) marls and calcarenites of the Cerda-Roccapalumba Formation (Triassic); 7) alluvial fan; 8) pond dam; 9) thrust; 10) tear fault; 11) attitude of strata; 12) normal crack within the landslide mass; 13) inverse crack within the landslide mass; 14) crack within the landslide mass; 15) strike-slip crack within the landslide mass; 16) aqueduct; 17) borehole; 18) recording station for ambient noise; 19) station of the temporary velocimetric array; 20) trace of geological section; 21) trace of seismic array; 22) supposed top of the Cerda-Roccapalumba calcarenites and marls in the geological section; 23) kinematical indicators for tear faults in the geological section (a – left fault, b – right fault); 24) supposed bottom of the Imera River alluvial deposits in the geological section; 25) supposed thickness of the Argille Varicolori scaly clays in the geological section.

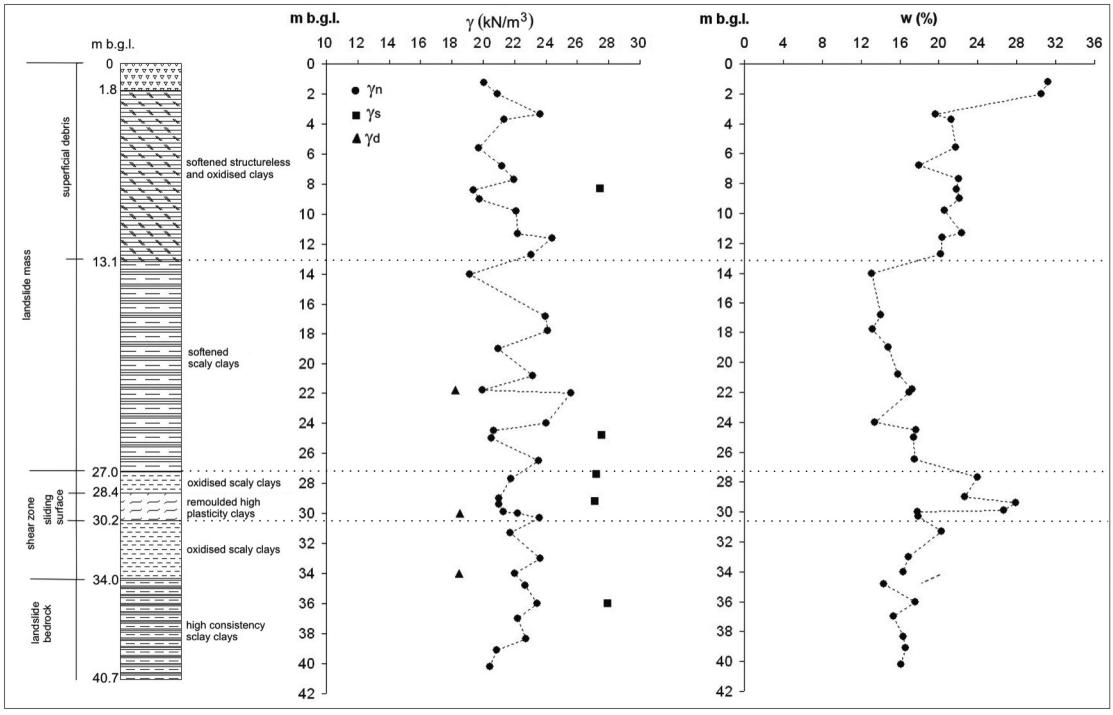

Fig. 5 - S2 borehole stratigraphy and variation with depth of the natural water content (w%) and of the natural unit weight volume (γ_n), compared with the solid unit weight volume (γ_s) and the dry unit weight volume (γ_{dry}).

4. Engineering-geology model of the Cerda landslide

The Cerda landslide (Fig. 4) mainly involved scaly clays belonging to the Argille Varicolori Formation (Cretaceous-Eocene) and including calcarenites of the Polizzi Formation (Eocene-Oligocene). The Argille Varicolori Formation overthrusts Triassic marls and limestones (Cerda-Roccapalumba Formation), widely outcropping in a tectonic window southeastward of the Cerda landslide (Abate *et al.*, 1988). The thrust limits the right side of the landslide mass, clarely corresponding to a creek. The same thrust is offset by numerous tear faults; one of them partly corresponds to the main scarp of the landslide.

The above-described structural setting is an open, basin-like structure of the Cerda landslide subsurface, characterised upslope by a high-angle lateral boundary and an irregular bedrock top, gently dipping downhill (see geological section in Fig. 4).

A first field investigation campaign (Bonci *et al*., 2004), included borehole S1 (Fig. 4) drilled down to 70 m b.g.l. close to the landslide crown area. In the S1 borehole, the rupture surface, corresponding to a 3-m thick layer of reddish and remoulded high plasticity clay, was observed at about 10 m b.g.l.. Results from laboratory characterisation of some samples taken from borehole S1 show a peak in clay content as well as in the plasticity index (PI) for the sample corresponding to the shear zone (Bonci *et al*., 2004). Another borehole (S2) was drilled within the landslide mass, about 300 m downhill from the previous one (S1). The stratigraphy shows an

11-m thick superficial layer of structureless and oxidised clay, a 14-m thick layer of softened scaly-clay, a 7-m thick layer of oxidised softened scaly clay including a 2-m thick layer of reddish remoulded clay, very similar and well correlated with the high plasticity clay level found in the S1 borehole 10 m b.g.l. (Fig. 5).

These results define a 30-m thick landslide mass, characterised by a moisture content between 12-20% (up to 30% in the first 2 m b.g.l.). The sliding surface corresponds to the reddish remoulded clay including lythorelicts, with a 9% moisture content increase with respect to the underlying and overlaying soils (Fig. 5). Even if no historical documents testify past activations of the Cerda landslide, both thickness and oxidation of the clayey remoulded shear zone testify its recurrent activity.

The depth of the sliding surface, inferred from borehole data, fits with the geological model of the landslide, derived from the observed ground crack pattern (Fig. 4). In particular, a mainly translational movement can be identified, with a downhill increasing thickness of the landslide mass, up to 60 m, different from what has been inferred by other authors (Agnesi *et al*., 2005), relating a deeper sliding surface to rotational sliding components. The analysis of the kinematic indicators within the landslide mass show notable differentiations that can be schematically referred to three zones (Figs. 3 and 4):

1) upslope section: cracks that opened up to 1 m, deepening to 4-5 m and evidence of deformations connected with tensile stresses;
2) midslope section: evidence of segmented strike-slip cracks with relative horizontal displacement, angular ramifications and local bulges;
3) downhill section: compressive cracks testified by evidence of soil bulging.

5. Geophysical Investigations

A combined geophysical approach was applied, to investigate the dynamic behaviour of the earthslide at low strain level as well as the landslide mass seismic amplification. The near-surface deposits involved in the landslide mass, were investigated by active seismic prospecting using both cross-hole and surface seismic techniques. On the other hand, passive seismic surveys were performed to point out possible amplification effects using both HVSR spectral ratios of ambient noise and weak motion records.

5.1. Active seismic prospecting

The purpose of active seismic prospecting is twofold. First, to provide a geometrical reconstruction of the near-surface deposits; second, to determine their dynamic elastic properties. Due to the landslide size, site S2 (Fig. 4) was selected for accurate determination of the dynamic elastic properties by means of seismic cross-holes. Then, aiming at investigating broader volumes of soil, several MASW (Park *et al*., 1999) surveys were performed along the landslide extent, to assess the shear-wave velocity profile in selected areas of the landslide body.

5.1.1. Cross-hole seismics

The P-wave and S-wave velocities were determined using different field geometries of shots and receivers. Data were acquired using a sparker down-hole source, capable of maximizing the

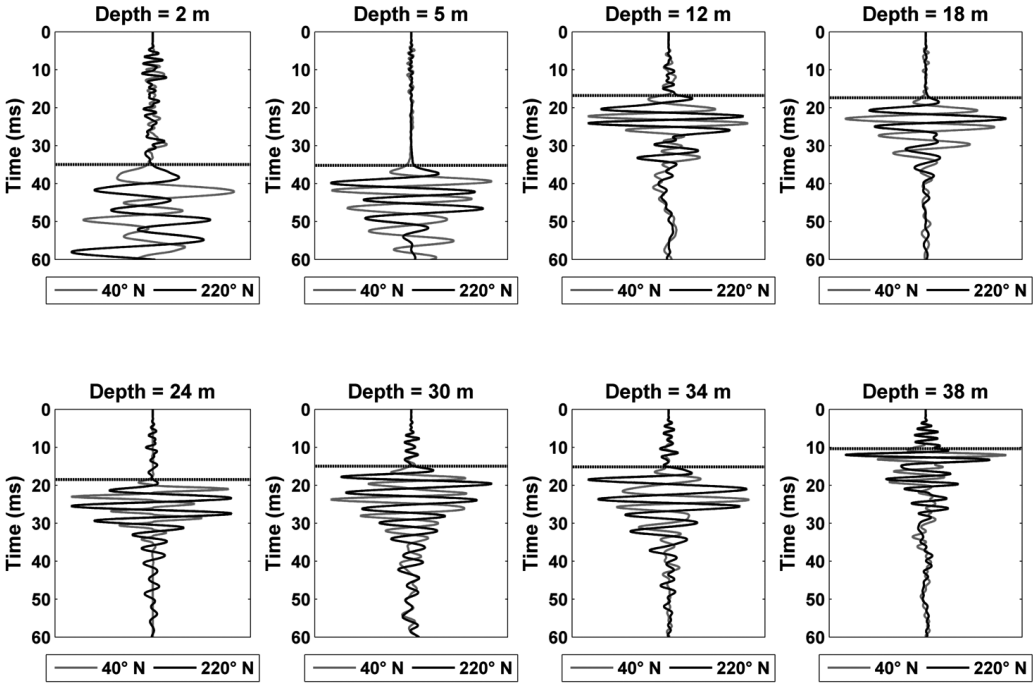

Fig. 6 - Example of cross-hole seismograms at selected depths along the borehole (transverse component). Black and grey traces represent opposite shots.

generation of either P waves or polarized SH waves. In order to maximize the SH wave generation some additional components are assembled with the basic P-wave sparker: a high impedance steel tube, a down-hole magnetic compass and a pneumatic clamping device. The steel tube, mounted on the sparker, has a long side window which allows the axial pressure pulse to be converted and focused on the horizontal direction. When the probe is pressed into the borehole walls by the pneumatic packer, this generates a horizontal shear motion in the ground. The so generated shear wave can be polarized according to the user's needs depending on the strike direction (i.e. on the position of the long side window), which can be controlled using the embedded down-hole compass.

As usual, in cross-hole seismic profiling (ASTM, 2000) source and geophones are positioned at the same elevation and, for each investigation depth, SH waves polarized in opposite directions (180°) are excited to read the S-wave first arrival by phase opposition. In this survey, a vertical spacing of 1 m was adopted; example seismograms extracted at significant depths along the borehole are reported in Fig. 6.

The complete S-wave profile is reported in Fig. 7: the V_S error bars associated with each elevation were calculated as r.m.s. of the repeated measurements or inferred from picking the uncertainty, considering also the possible errors arising from hole deviation.

The P-wavefield was analyzed in 2D using a tomographic approach. Fig. 8 shows the source-receiver layout and the P-wave velocity model assessed by inversion, using the algorithm described in Bernabini and Cardarelli (1997), which assumes straight ray-path approximation.

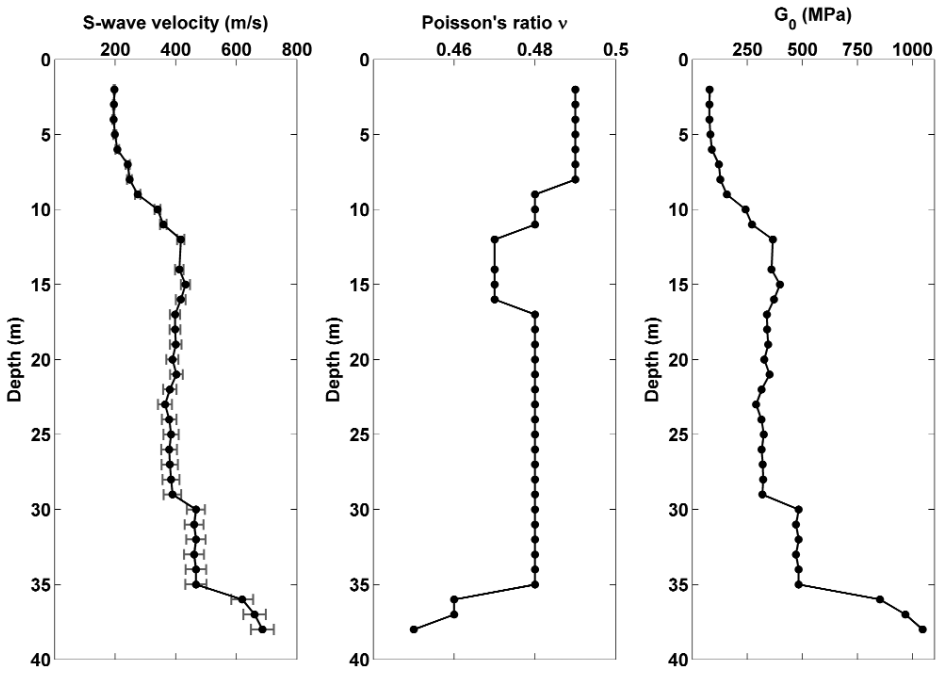

Fig. 7 - Left: the S-wave velocity profile from cross-hole data at site S2. Center: Poisson's ratio vs. depth. Right: elastic shear modulus vs. depth.

A P-wave velocity model and an S-wave velocity profile show excellent agreement with borehole stratigraphy. In particular, in terms of V_S, a low-stiffness stratum (6 m) of about 200 m/s, gradually passing to 400 m/s at about 13 m, was determined. Below this level, the shear-wave velocity remains approximately constant down to the supposed sliding surface (about 30 m b.g.l.). Below this depth, V_S is increasing to about 500 m/s down to 35 m b.g.l., where it sharply reaches values of about 700-750 m/s. At this depth range, high consistency scaly clay was recovered by drilling.

Poisson's ratio and the elastic shear modulus G_0 were derived from the compressional (P) and shear (S) wave velocities (Fig. 7), using values of mass density independently measured by field laboratory tests (Fig. 5).

5.1.2. MASW survey

MASW (Park *et al*., 1999) surveys were also performed to investigate the S-wave velocities of larger volumes of the landslide mass.

Surface wave data were acquired at different (and symmetric where possible) offsets, using 48 vertical 4.5 Hz geophones. Uniform geophone spacing was used (2 or 3 m, depending on the line). Each shot gather was pre-processed (air-wave and first arrival muting, low-pass filtering, bad traces elimination) then transformed in the f-c (frequency-phase velocity) domain (Park *et al*., 1998) for dispersion curve evaluation. For each seismic line, all the picked dispersion curves were used to build the mean dispersion curve from the ensemble, determining also the statistical

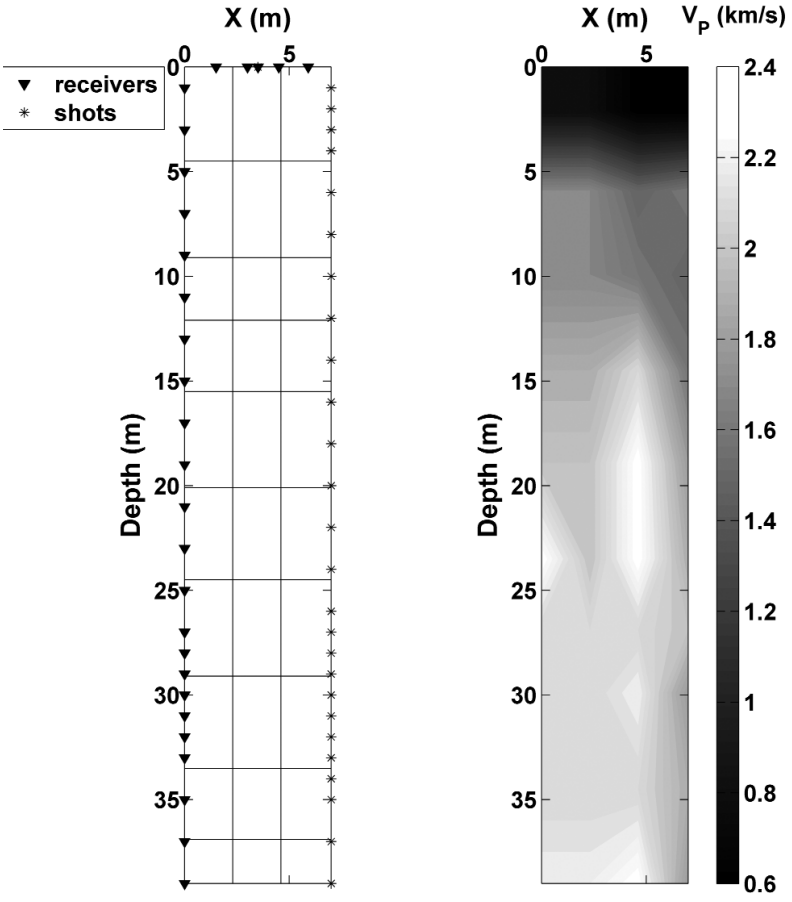

Fig. 8 - Left: configuration of source and receivers for seismic tomography, together with model cell display. Cell discretisation was selected on the basis of the Fresnel ray theory. Right: the VP-section inferred from tomographic inversion.

distribution of experimental errors (r.m.s.), once a Gaussian distribution was assumed.

Due to moderate lateral variation of seismic velocity within the landslide, 1D MASW interpretation represents a reasonable assumption.

Dispersion curves were inverted using inequality-constraint damped least squares inversion (Cercato, 2007). Fig. 9 reports the profiles associated with distinct seismic arrays. The retrieved V_S values do not differ significantly among the lines and are in good agreement with the cross-hole seismic profile (Fig. 9, top).

5.2. Seismometric records

A velocimetric survey was carried out to analyse the local seismic response inside and outside the landslide area. A moving station, equipped with a digital acquisition unit (K2 Kinemetrics) and three short-period sismometers (SS1 Kinemetrics) triaxially arranged (NS-UP-WE), was used to record ambient noise samples. The spatial distribution of the measurement sites was planned according to the known geomorphological features, the location of the boreholes as well as proper settlement conditions (SESAME, 2004) a good coverage of the area.

The recording stations were located all over the involved slope (Fig. 10), both inside the

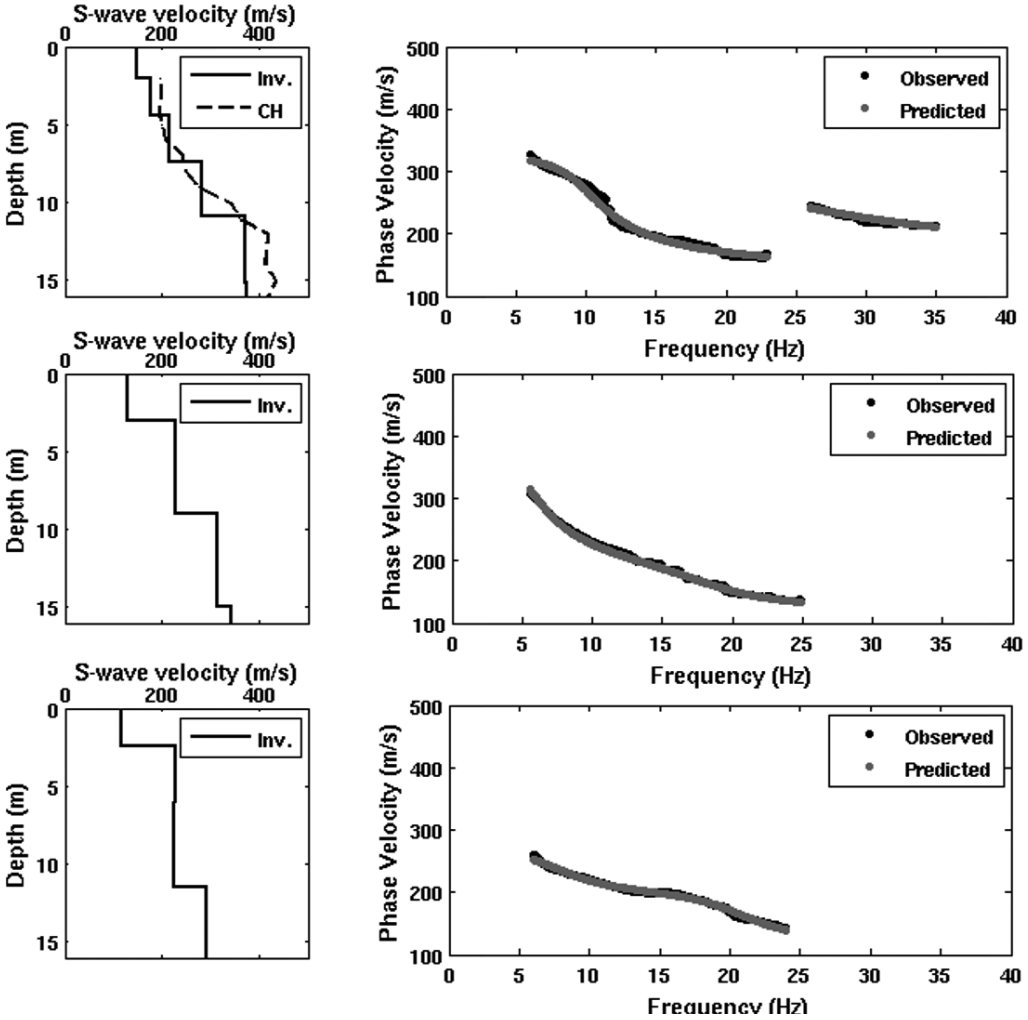

Fig. 9 - Results of MASW inversion. Top: Line1 – 0-141 m. Center: Line1 – 141-242 m. Bottom: Line 2.

landslide mass (in the detachment area, in the toe area, in the neutral zone and along the flanks) and outside the landslide (alluvial deposits of the Imera River, the Argille Varicolori Formation and limestones of the Cerda-Roccapalumba).

Overall, ambient noise records of 15 minutes were measured in 36 sites and further processed according to the HVSR technique (Nakamura, 1989). The records were sampled with a 40 s moving time window and FFT transformed into the frequency domain to get the average spectra of the 3 components (NS, UP, WE) for each station, and the NS/UP, WE/UP spectral ratios. Starting from these preliminary results, at least a second noise record was acquired during the night at the sites where amplification effects had been observed.

The HVSR spectral ratios of the two horizontal components obtained in each station were compared; since no main directional effect was identified, the average HVSR ratio was taken into account. For all the analyses, only the HVSR values larger than 2 were considered, in agreement

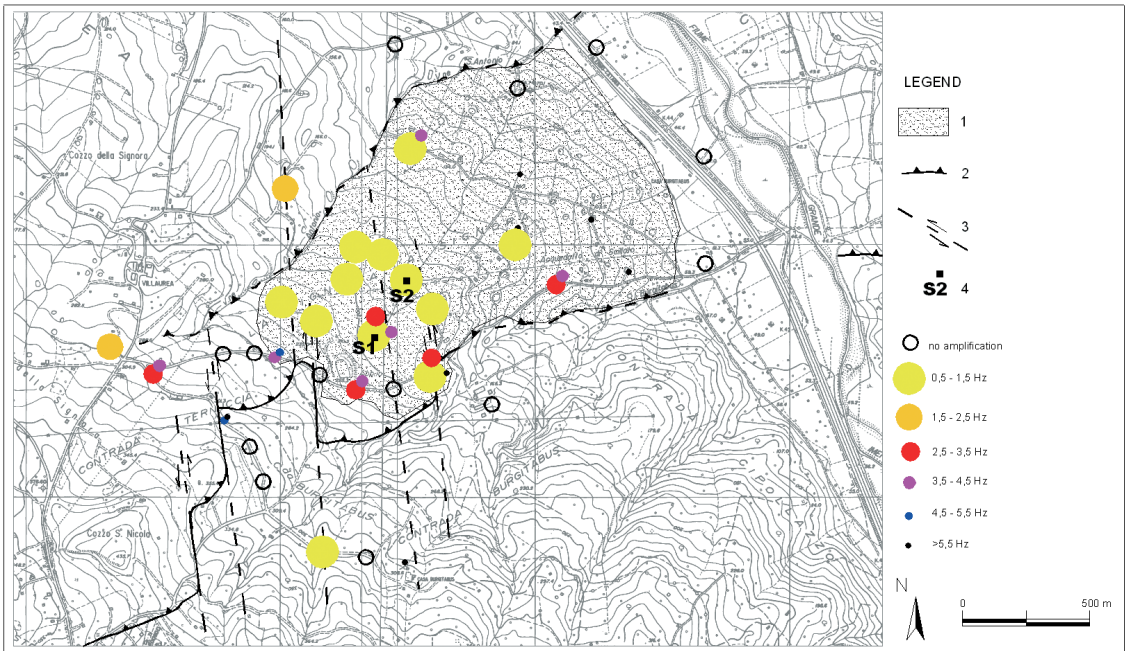

Fig. 10 - Amplification frequencies from HVSR in the Cerda landslide area; circles mark the recording stations for ambient noise, while squares mark the temporary velocimetric array stations: 1) thrust; 2) tear fault; 3) landslide scarp; 4) inverse crack; 5) strike-slip crack; 6) crack; 7) bulge area.

with the SESAME (2004) standards.

While noise measurements were performed, a temporary velocimetric array was deployed to record possible small-magnitude events. Four free-field stations, each one instrumented with a K2 digital acquisition unit, three SS1 sismometers and GPS for absolute timing, operated for 10 days (June 24 to July 2) in STA/LTA (Short Time Amplitude/Long Time Amplitude) acquisition mode.

The array locations (Fig. 10) were selected according to both previously collected geological data and preliminary noise analysis. One station (R1) was positioned outside the landslide mass, on the limestones of the Cerda-Roccapalumba Unit, on a flat site with no evidence of intense rock mass jointing. Given these features, the site is considered representative of the local seismic bedrock and can be therefore assumed as a reference station according to Borcherdt (1994). The other stations were located on the landslide mass: two (S1, S2) were placed near drillings S1 and S2, where borehole stratigraphy as well as geotechnical and geophysical data had been collected previously; the last one (C) was placed in the "neutral zone" of the landslide in order to monitor

Table 2 – Setting parameter of Kinemetrics-K2 acquisition unit.

Pre event time	Post event time	STA	LTA	STA/LTA	STA/LTA filter frequency range
15 s	15 s	1 s	60 s	4	1-10 Hz

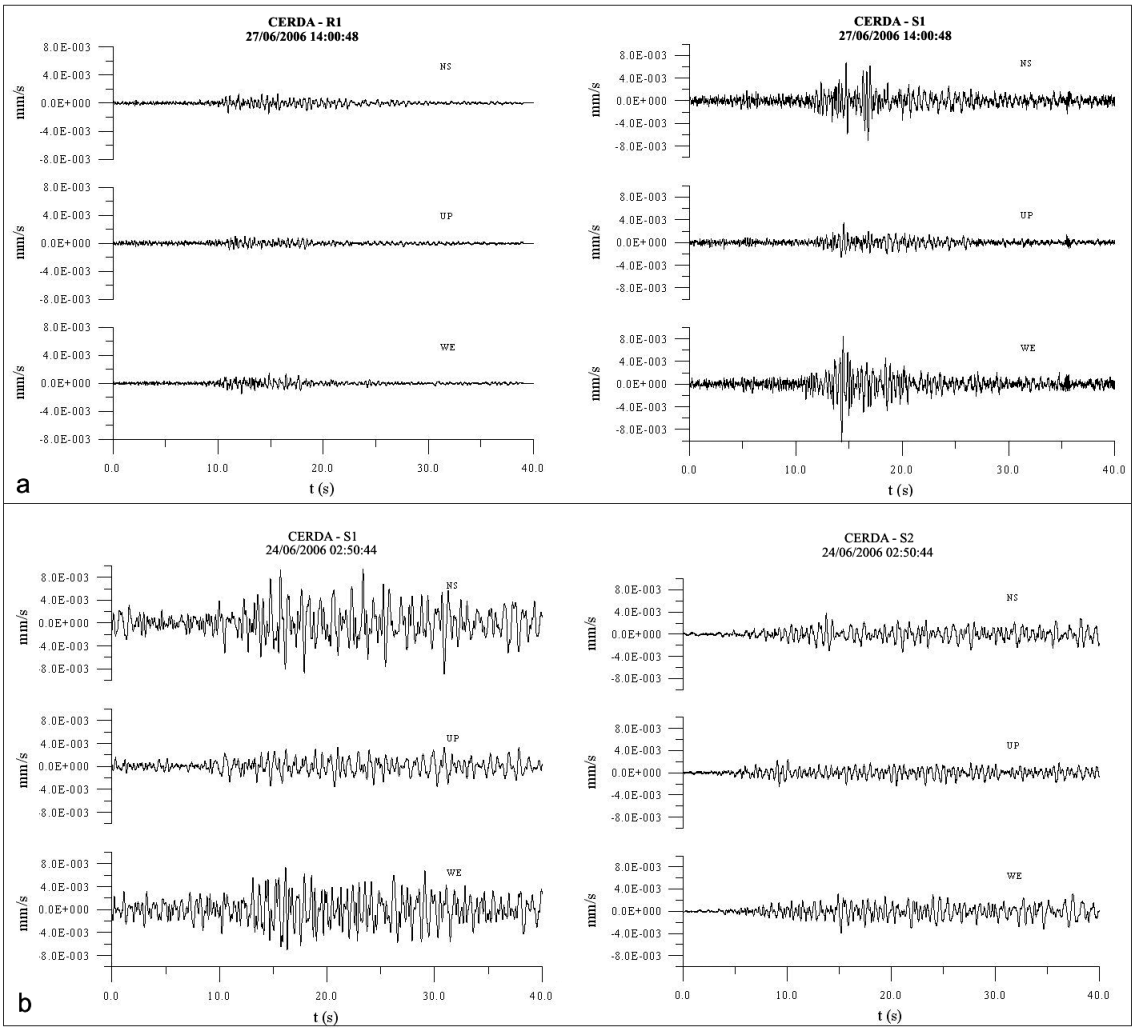

Fig. 11 - a) Time histories of the June 27, 2006 earthquake recorded at stations S1 and R1; b) time histories of the June 24, 2006 earthquake recorded at stations S1 and S2.

the behaviour of different landslide sectors. Since it did not show any amplification effect, this station was moved outside the landslide mass, on the Argille Varicolori Formation (R2).

The acquisition settings, reported in Table 2, were selected taking into account the main

Table 3 – Earthquakes recorded by the temporary array stations.

date	time	triggered stations	MI	epicentre
24/06/2006	02.50.44	S1, S2	n.a.	n.a.
27/06/2006	14.00.48	S1, R1	2.8	Eolie

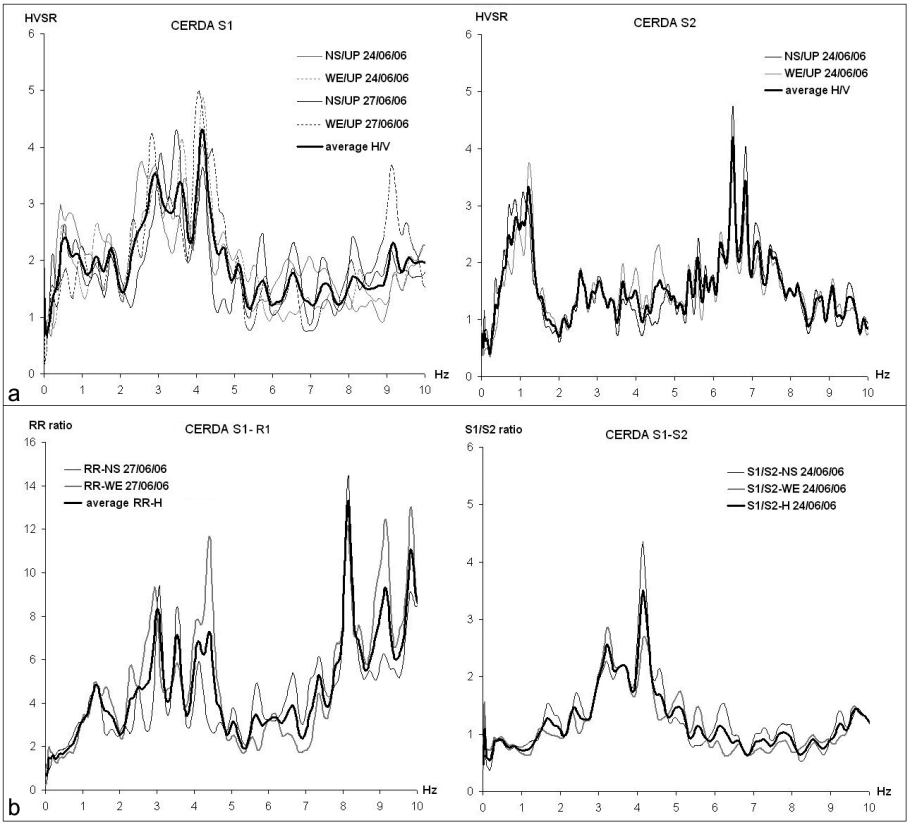

Fig. 12 - a) Receiver functions at stations S1 and S2 obtained from the recorded earthquakes; b) Spectral ratios of the horizontal components recorded at the S1 station to the corresponding components recorded at the reference station (left); Spectral ratios of the horizontal components recorded at the S1 station to the corresponding components recorded at the S2 station (right).

seismic features of the site; the STA/LTA rate of station R1 was reduced to 3, after observing that it had not been triggered by a weak motion event recorded at other stations.

Only 2 weak motion events were recorded by some stations of the temporary array (Table 3). The June 27, 2004 earthquake (M_L=2.8) was located by INGV, in the Aeolian Islands source (INGV, 2002). The records (Fig. 11) obtained for these events were FFT transformed adopting the same spectral smoothing used for noise data.

Given the insufficient number of weak-motion data, the analysis of the seismic response was based on the noise records. The significant values were clustered into 6 frequency classes in the range 0.5-6.5 Hz; the results are reported in Fig. 10 for each recording station where also stations that did not amplify are reported.

The HVSR ratios point to a wide amplificating zone in the range 0.5-1 Hz within the landslide mass, in the upper part of the slope (stations 8, 9, 15, 16, 17, 30, S2, S1) close to the high-angle fault contact (Bonci *et al.*, 2004) between the Cerda Roccapalumba and the Argille Varicolori Formations (Fig. 4). Along the landslide perimeter zone, the amplified frequencies are in the

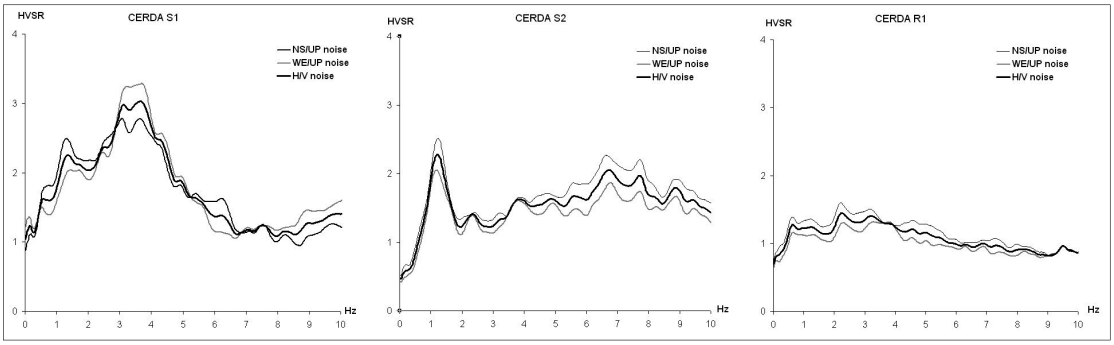

Fig. 13 - Average HVSR from noise records obtained at stations S1, S2 and R1.

range 2.5-4.5 Hz (stations 7, 11, 13 20, 23), while they reach values of up to 7.5 Hz inside the landslide mass, in correspondence with its toe (stations 21, 22, 24). Other amplification effects were observed outside the landslide mass along intensely-jointed fault zones (stations 1, 2, 18, 29, 31); these effects might be related to trapped modes due to adjacent rock masses with very different jointing conditions (Martino *et al*., 2006) (Fig. 10). No amplification effects appear in the Imera River alluvial deposits (stations 25, 26, 27).

Starting from the FFT of the recorded weak motions, the receiver functions (Field and Jacob, 1995) were obtained in the related stations (Fig. 12a). Only for the second event, was it possible to compute the spectral ratio of S1 to the reference station (Borcherdt, 1994) (Fig. 12b). The results are consistent with those obtained from the HVSR of ambient noise (Fig. 13). Moreover, the spectral ratio between the horizontal components recorded at the S1 and S2 stations, obtained for the June 24, 2006 earthquake, highlights a relative amplification, closer to the detachment area of the landslide, of ground motion in S1, in the 3-5 Hz range (Fig. 12b).

6. Remarks

The Cerda landslide is an earthslide with a mainly translational mechanism, which involved scaly clays of the Argille Varicolori Formation. The geological section and the kinematical evidence, according to geophysical surveys and borehole data, show a shear zone with a thickness varying from some meters in the crown area up to 60 m at the toe (Figs. 2 and 14). P-wave tomography was not capable to discriminate between landslide mass and its geological bedrock. On the other hand, seismic prospecting based on S-wave velocity pointed out a consistent lateral uniformity of the elastic stiffness properties at low strain and a shear-wave stratification which confirms a kinematical layering of the landslide mass. Gradually increasing velocity values were recorded in a 13-m-thick superficial remoulded layer; on the contrary, a nearly constant V_S value exists between 13 and 30 m b.g.l. at S2 location. The seismic wave velocity values sharply increase below the supposed landslide shear zone (about 32 m b.g.l.), in correspondence with the landslide mass substratum, composed of high consistency and structured scaly clays (Fig. 5). This two-layer geomechanical and physical model of the Cerda landslide mass, due to the presence of

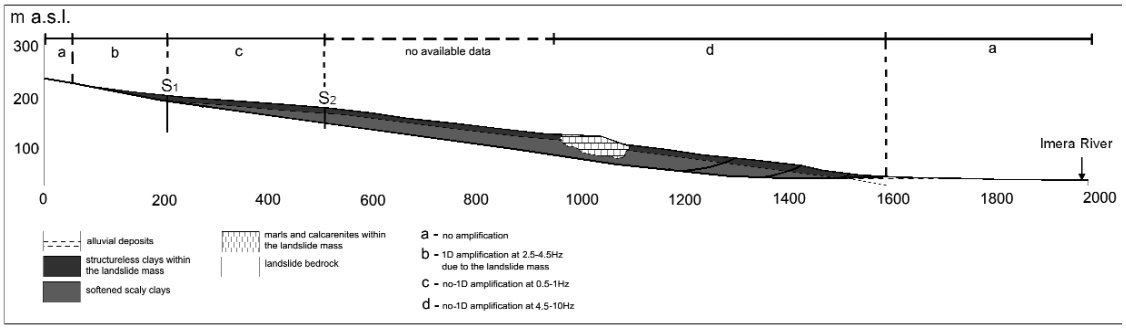

Fig. 14 - Engineering-geology sketch of the Cerda landslide and distribution of the observed amplification effects.

highly disturbed and remoulded clays in its superficial portion, can be responsible for a multifrequency resonance effect; in this case, only the lowest frequency peaks should be converted into depths in order to obtain an actual shape of the sliding surface (Meric *et al*., 2007). Nevertheless, the resulting depths have to be validated by both the geomechanical and the kinematical evidence collected in the landslide area.

The seismometric measurements of both ambient noise and weak motion, performed in the Cerda landslide area, showed possible local seismic amplification effects (Fig. 10).

The distribution of the picked frequencies, that were obtained from the HVSR spectral ratios, show a significant variation within the landslide mass area:

1) an amplification in the range 2.5-4.5 Hz, also confirmed by the analysis of two weak-motion records measured at S1 station, appears inside the landslide mass and along its perimeter zone; this frequency range, given the shear wave velocity measured in the landslide mass (varying from 200 to 400 m/s), can be referred to the 1D resonance frequency of the landslide mass thickness;
2) the observed 0.5-1.5Hz frequency peak, which uniformly characterises the upslope portion of the landslide, cannot be referred to a 1D resonance effect of the landslide mass since, in this portion of the slope, the observed depth of the sliding surface reaches 30 m. On the other hand, taking into account the fact that in the same portion of the slope the depth of the marly and calcarenitic bedrock is about 150 m b.g.l., the corner geometry, generated by near lateral discontinuities corresponding to the contact scaly clay-geological bedrock, can be considered responsible for this effect (Mozco and Bard, 1993);
3) no significant amplification effects are measured in the lower portion of the slope, at the toe of the landslide, where a more disturbed and heterogeneous clay material, involved in flow-type movements, is present. This corresponds to a less significant S-wave contrast at the bottom of the landslide mass in agreement with Meric *et al*. (2007).

As reported in Fig.15, the Cerda landslide is plotted well beyond the upper bound defined by the curve of the maximum distance for coherent landslide activation by Rodriguez *et al*. (1999), since it has a large epicentral distance (about 50 km) if compared with the magnitude of the Palermo earthquake (M_S=5.4). Actually, a low intensity value [V MCS according to Azzaro *et al*.

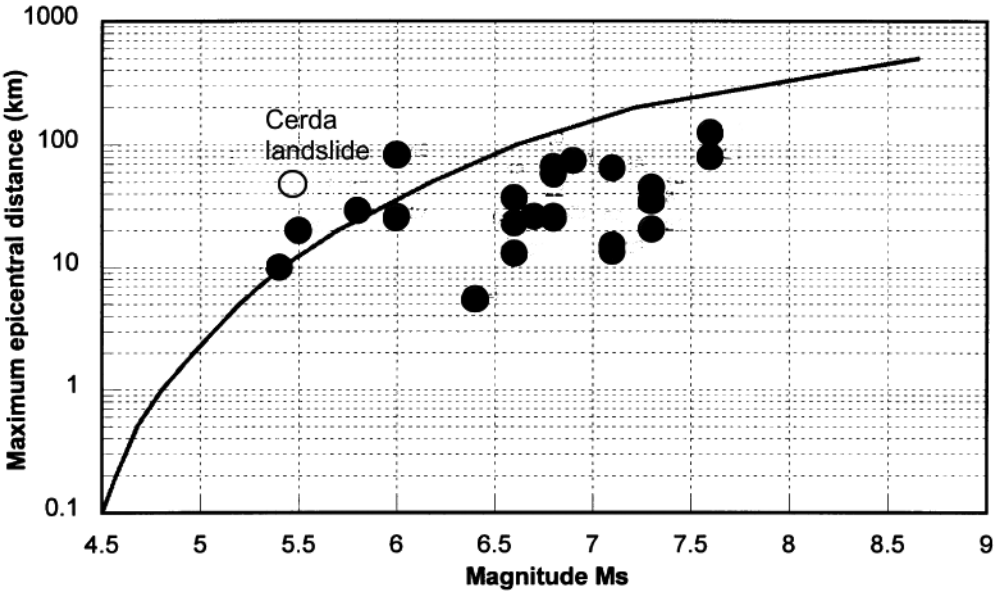

Fig. 15 - Maximum epicentral distance versus magnitude for seismic trigger of coherent landslides [modified from Rodriguez *et al*. (1999)].

(2004)] was assessed for the village of Cerda, a few kilometres from the landslide area, on account of the 2002 earthquake.

A conventional Newmark (1965) analysis was also performed on the basis of the geometrical and geotechnical properties of the landslide mass. In agreement with the far-field location of the Cerda landslide, an expected displacement <<1 cm was computed for the landslide mass the applying the function by Romeo (2000):

$$\log_{10} D \text{ (cm)} = -1.281 + 0.648M_L - 0.934\log_{10}(RE^2 + 3.5^2)^{1/2} - 3.699K + 0.225S \pm 0.418$$

where D=expected displacement, M_L=earthquake local magnitude=5.6, RE=epicentral distance=50 km, K=critical acceleration ratio=0.97, S=soil coefficient=1. In particular, the K coefficient (=kc/PGA) was computed by assuming an expected PGA=0.175 g [PGA expected to be exceeded at 10% probability level in 50 years, according to the Gruppo di Lavoro (2004)] and a critical pseudostatic coefficient kc=0.17g, derived from the relation by Jibson (1993):

$$kc = g \tan(\phi - \beta)$$

where g=9.81 m/s^2; ϕ=residual friction angle along the sliding surface=16° and β=average dip of the slope=10°.

The so-computed Newmark co-seismic displacement value for the Cerda landslide highly underestimates the measured ones, which reach some meters in the detachment area and some tens of centimetres at the bottom of the slope.

From collected evidence, it can be inferred that local conditions due to a much more complex landslide-earthquake interaction have to be considered in order to justify the far-field 2002 reactivation of the Cerda landslide. These interactions could be related to local seismic amplification effects as well as to the dynamic response of the clays involved in the landslide.

The present work gives new elements for analysing the possible role of the seismic input on the far field activation of the Cerda landslide, since the input frequency content, as well as its amplitude, can strongly control the dimension of the mobilised mass and the values of the induced displacements (Hutchinson, 1987; Martino and Scarascia Mugnozza, 2005). To this aim, the landslide mass itself, as well as the geological setting of the landslide area, were taken into account as possible source of local seismic amplification effects.

Seismic wave propagation as well as stress-strain dynamic 2D numerical modelling are under implementation in order to i) validate the above reported hypotheses on possible amplification due to both 1D and 2D effects, ii) obtain the amplification functions, iii) analyse the possible relations between the frequency content of the seismic input and the landslide trigger.

7. Conclusions

Detailed investigations were performed in the area of the Cerda landslide after its last reactivation (September 6, 2002) in order to define the engineering-geological model and eventually identify possible local seismic amplification effects. The engineering-geology and geophysical investigations pointed out a two-layer model as representative of the landslide mass, which is composed by superficial highly disturbed and remoulded clay, overlapping softened scaly-clay. Moreover, in the upper section of the slope, the sliding surface well corresponds with the measured scatter of the seismic wave velocities.

The seismometric records show some local seismic amplification effects within the landslide area. The engineering-geology model, confirmed by active seismic prospecting, demonstrates that they are due to the 1D resonance of the landslide mass itself along the landslide perimeter zone; the other observed amplification effects, however, cannot be related to 1D resonance.

The lack of significant amplification effects at the bottom of the slope can be related to a main flow-type movement of the landslide as well as to a more heterogeneous landslide mass.

Given the measured S-wave velocities within the first 30 m b.g.l (up to 400 m/s), the 1D resonance frequency (2.5-4.5 Hz) can be referred to the landslide thickness, while the 1 Hz amplification effect could be related to the structural setting of the geological bedrock.

Acknowledgement. The authors wish to thank F. Lucenti (co-operator, University of Rome “La Sapienza”, Dipartimento di Scienze della Terra) and F. Pugliese (technician, University of Rome “La Sapienza”, Dipartimento di Idraulica Trasporti e Strade, Area Geofisica) for their contribution during the field activities, E. Esposito and S. Porfido (CNR - I.A.M.C.) for their personal communications about historical seismicity and D. Jongmans (LIRIGM, Grenoble) for the useful discussions on the collected data. The research was funded by grant PRIN2005, project title: “Induced seismic hazard: analysis, modelling and predictive scenarios of earthquake triggered landslides” (resp. G. Scarascia Mugnozza).

REFERENCES

Abate B., Renda P. and Tramutoli M.; 1988: *Schema geologico dei Monti di Termini Imerese e delle Madonie Occidentali (Sicilia)*. Mem. Soc. Geol. It., **41**, 465-474.

Agnesi V., Camarda M., Conoscenti C., Di Maggio C., Diliberto I.S., Madonia P. and Rotigliano E.; 2005: *A multidisciplinary approach to the evaluation of the mechanism that triggered the Cerda landslide (Sicily, Italy)*. Geomorphology, **65**, 101-116.

Asten M.W.; 2004: *Passive seismic methods using the microtremor wave field for engineering and earthquake site zonation*. In: Proc. 74th SEG Annual Meeting, Denver, USA, Session NGS-1.

ASTM; 2000: *Standard D-4428/D-4428M-00, "Standard Test Methods for Crosshole Seismic Testing"*. American Society for Testing Materials.

Azzaro R., Barbano M.S., Camassi R., D'Amico S., Mostaccio A., Piangiamore G. and Scarfì L.; 2004: *The earthquake of 6 September 2002 and the seismic history of Palermo (Northern Sicily - Italy): implications for the seismic hazard assessment of the city.* Journal of Seismology, **8,** 525-543.

Bard P. and Bouchon M.; 1985: *The two-dimensional resonance of sediment-filled valleys.* Bull. Seism. Soc. Am., **75**, 519–541.

Bernabini M. and Cardarelli E.; 1997: *Variable damping factors in traveltime tomography.* Journal of Applied Geophysics, **38**, 131–141.

Bonci L., Bozzano F., Calcaterra S., Eulilli V., Ferri F., Gambino P., Manuel M.R., Martino S. and Scarascia Mugnozza G.; 2004: *Geological control on large seismically induced landslides: the case of Cerda (Southern Italy).* In: Proc. IX ISL, Rio de Janeiro, pp. 985-991.

Borcherdt R.D.; 1994: *Estimates of site-dependent response spectra for design (methodology and justification)*. Earthquake Spectra, **10**, 617-653.

Bordoni P., Cara F., Cercato M., Di Giulio G., Haines A.J., Milana G., Rovelli A. and Ruso S.; 2006: *The use of a very dense seismic array to characterize the Cavola (Northern Italy) active landslide body.* In: ESG Third International Symposium on the Effects of Surface Geology on Seismic Motion, Grenoble August 30 - September 1 2006, Poster session

Chavez-Garcia F.J.; 2007: *Site effects: from observation and modelling to account for themin building codes.* In: Pitilakis K.D. (ed), Earthquake Geotechnical Engineering, Proc. 4th International Conference on Earthquake Geotechnical Engineering, Springer, pp. 53-72.

Cercato M.; 2007: *Linearized inversion of MASW data using inequality constraints.* In: EAGE Near Surface 2007, Extended Abstracts, B15.

CFTI3; 2000: *Catalogue of strong Italian earthquakes from 461 a.C. to 1997*. ING-SGA, Bologna.

CPTI04; 2004: *Catalogo Parametrico dei Terremoti Italiani dal 217 a.C. al 2002*. INGV, website http://emidius.mi.ingv.it/CPTI04/.

Cruden D.M. and Varnes DJ.; 1996: *Landslide types and processes.* In: Turner A.K., Schuster R.L. (eds), Landslides: investigation and mitigation, Transportation Research Board, Spec. Report 247, National Research Council, National Academy Press. Washington DC, pp. 36–75.

DBMI04; 2004: *Database Macrosismico Italiano.* INGV, website http://emidius.mi.ingv.it/DBMI04.

Field E.H. and Jacob K.; 1995: *A comparison and test of various site response estimation techniques, including three that are not reference-site dependent.* Bull. Seism. Soc. Am., **85**, 1127-1143.

Fookes P.G., Baynes F.J. and Hutchinson J.N.; 2000: *Total geological history: a model approach to the anticipation, observation and understanding of site conditions.* In: GeoEng 2000, International Conference on Geothecnical and Geological Engineering, Melbourne, pp. 370-460.

Gallipoli M., Lapenna V., Lorenzo P., Mucciarelli M., Perrone A., Piscitelli S. and Sdao F.; 2000: *Comparison of geological and geophysical prospecting techniques in the study of a landslide in southern Italy*. European J. Env. Eng. Geophys., **4**, 117–128.

Gruppo di Lavoro; 2004: Redazione della Mappa di Pericolosità Sismica prevista dall'Ordinanza del 20/03/2003 n. 3274 All. 1, per il Dipartimento di Protezione Civile, INGV, Milano-Roma, April 2004, 65 pp.+ 5 annexes.

Havenith H.B., Jongmans D., Faccioli E., Abdrakhmatov K. and Bard P.Y.; 2002: *Site effect analysis around the seismically induced Ananevo rockslide, Kyrgystan.* Bull. Soc. Seism. Am., **92**, 3190-3209.

Havenith H.B., Vanini M., Jongmans D. and Faccioli E.; 2003: *Initiation of earthquake-induced slope failure: influence of*

topographical and other site specific amplification effects. Journal of Seismology, **7**, 397-412.

Hutchinson J.N; 1987: *Mechanism producing large displacements in landslides on pre-existing shears.* Mem. Soc. Geol. of China, **9**, 175-200.

INGV; 2002: *Bollettino della Sismicità strumentale*, ftp://ftp.ingv.it/bollet/.

Jibson R.W.; 1993: *Predicting earthquake-induced landslide displacement using Newmark sliding block analysis.* In: Transportation Research Board, National Research Council, Washington D.C., TR record 1411, pp. 9-17.

Jongmans D. and Garambois S.; 2007: *Geophysical investigation of landslides: a review.* Bull. Soc. Géol. Fr., **178**, 101-112.

Keefer D.K.; 1984: *Landslides caused by earthquakes.* Geol. Soc. Am. Bull., **95**, 406-421.

Marcelli L. and Spadea M. C.; 1981: *La profondità ipocentrale con metodi macrosismici.* Ann. Geof., **34**, 5-36.

Martino S. and Scarascia Mugnozza G.; 2005: *The role of the seismic trigger in the Calitri landslide (Italy): hystorical reconstruction and dynamic analysis.* Soil Dynamic Earthquake Engineering, **25**, 933-950.

Martino S., Minutolo A., Paciello A., Rovelli A., Scarascia Mugnozza G. and Verrubbi V.; 2006: *Seismic microzonation of jointed rock-mass ridges through a combined geomechanical and seismometric approach*. Natural Hazards, **39**, 419-449.

Meric O., Garambois S., Jongmans D., Wathelet M., Chatelain J.L, and Vengeon J.M.; 2005: *Application of geophysical methods for the investigation of the large gravitational mass movement of Séchilienne, France*. Can. Geotech. J., **42**, 1105–1115.

Méric O., Garambois S., Malet J.P., Cadet H., Guéguen P. and Jongmans D.; 2007: *Seismic noise-based methods for soft-rock landslide characterization.* Bull. Soc. Géol. Fr., **178**, 137-148.

Mozco P. and Bard P.Y.; 1993: *Wave diffraction, amplification and differential motion near strong lateral discontinuities.* Bull. Seism. Soc. Am., **83**, 85-106.

Nakamura Y.; 1989: *A method for dynamic characteristics estimation of subsurface using microtremor on the ground surface*. QR of RTRI, **30**, 25-33.

Newmark N.M.; 1965: *Effects of earthquakes on dams and embankments.* Geotechnique, **15**, 139-159.

Nunziata C.; 2007: *A physically sound way of using noise measurements in seismic microzonation, applied to the urban area of Napoli.* Engineering Geology, **93**, 17-30.

Park C.B., Miller R.D. and Xia J.; 1998: *Imaging dispersion curves of surface waves on multichannel records.* In: 68th SEG Meeting Expanded Abstract, pp. 1377-1380.

Park C.B., Miller R.D. and Xia J.; 1999: *Multichannel analysis of surface waves*. Geophysics, **64**, 800-809.

Rodriguez C.E., Bommer J.J. and Chandler R.J.; 1999: *Earthquake-induced landslides: 1980-1997.* Soil Dynamics and Earthquake Engineering, **18**, 325-346.

Romeo R.: 2000: *Seismically induced landslide displacements: a predictive model.* Engineering Geology, **58**, 337-351.

Roten D., Cornou C., Steimen S., Faeh D. and Giardini D.; 2004: 2*D resonances in Alpine valleys identified from ambient vibration wavefield.* In: Proc. 13th World Conf. Earth. Eng., Vancouver, Canada. – IAEE., Tokyo, paper 1787.

Rovelli A., Caserta A., Marra F. and Ruggiero V; 2002: *Can seismic waves be trapped inside an inactive fault zone? The case-study of Nocera Umbra, Central Italy.* Bull. Seism. Soc. Am., **92**, 2217–2232.

SESAME; 2004: *Guidelines for the implementation of the H/V spectral ratio technique on ambient vibrations.* Website http://sesame-fp5.obs.ujf-grenoble.fr/index.htm.

Shapiro N.M., Campillo M., Stehly L. and Ritzwoller M.; 2005: *High resolution surface wave tomography from ambient seismic noise.* Science, **307**, 1615-1618.

Steimen S., Fäh D., Kind F., Schmid C. and Giardini D.; 2003: *Identifying 2-D resonance in microtremor wave fields.* Bull. Seism. Soc. Am., **93**, 583-599.

Corresponding author: Salvatore Martino
Dip. Scienze della Terra
Università "La Sapienza"
P.le A. Moro 5, 00185 Roma, Italy
phone - fax: +39 06 49914923; e-mail: salvatore.martino@uniroma1.it